Disclaimer: This is not the final version of the article. Changes may occur when the manuscript is published in its final format.

Molecular Modeling Connect
ISSN: 3105-3734
2026, Vol. 3, Cite as: doi:10.x/journal.x.x.x

SCIFINITI PUBLISHING

OPEN ACCESS

Research Article

Computational Investigation of Selected Antivirals and mAbs Targeting the RBD of Omicron to Get Insights into Structure and Binding Attributes

Sudheer Kumar Katari[1*#], Kesavi HimaBindhu Vuyyuru[1], Anil Kumar Singh[2*#]

[1]Department of Biotechnology, Vignan's Foundation for Science, Technology and Research, Vadlamudi-522213, Guntur, India

[2]Academy of Scientific and Innovative Research (AcSIR), Ghaziabad-201002, India.

*Corresponding authors: katari319@gmail.com (S.K. Katari); phd.anil@yahoo.com (A.K.Singh);

Sudheer Kumar Katari: katari319@gmail.com

ORCID iD:- 0000-0002-4345-2141

Kesavi HimaBindhu Vuyyuru: vuyyurukesavihimabindhu@gmail.com

ORCID iD:-0009-0000-3030-8784

Anil Kumar Singh: phd.anil@yahoo.com

ORCID iD:- 0000-0002-5721-6502

Highlights

- Computational investigation revealed variability in the structure of VOCs spike proteins.
- Secondary structure elements exhibited variable constituent elements in a range of 3.54–46.84%
- Omicron-RBD binding with selected antiviral drugs was found to be acceptable binding affinity in a range of -5.2±0.26 to -7.4±0.06 Kcal/mol.
- Findings could be translated for further investigation by implementing an experimental assay.

Abstract

Multiple mutations in the nCoV have resulted in the emergence of a variant of concern (VOC). A mutation in the receptor-binding domain (RBD) often influences the virus interaction with cell surface receptors, pathogenicity, and evades immune response. Such VOCs pose a public health risk owing to their capacity to evade immune system responses, as well as variations in pathogenicity and transmissibility. In an effort to understand these challenges, we investigated the structure, function, and binding efficiency of RBDs of VOCs by implementing selected antiviral drugs and monoclonal antibodies (mAb). The secondary structural element (SSE) of spike protein (S) of VOCs was found to be 26.79-29.43% Alpha helix (Hh), 21.64-22.37% Extended strand (Ee), 3.54-5.12% Beta turn (Tt), and 45.40-46.84% random coil (Cc). Docking simulations revealed that the nCoV-RBD-Lopinavir complex exhibited the lowest binding affinity (-8.8±0.55 Kcal/mol), by forming H-bond interactions with ALA-27 and ALA-143 residues. Likewise, Omicron-

RBD- Indinavir complex exhibited the lowest binding affinity (-7.4 ±0.06 Kcal/mol), involving ARG-355, ASP-428, THR-430, SER-514, GLU-516 residues to form H-bond interactions. Protein-protein docking of Omicron RBD-ACE2 revealed a good score of -846.2 compared to the reference complex (-703.1). The findings presented herein explain the considerable structural and functional alterations in Omicron's RBD with reference to RBD (nCoV). This variation showcases the diverse binding affinities of selected antiviral drugs and mAb. The findings may pave the way for experimental validation, leading to a deeper understanding of potential therapeutic options against SARS-CoV-2 and similar diseases.

Keywords: receptor binding domain; spike protein; docking simulations; Omicron-RBD binding; variant of concern

1. Introduction

The Betacoronaviruses genus encompasses the severe acute respiratory syndrome coronavirus (SARS-CoV), Middle East respiratory syndrome coronavirus (MERS-CoV), and the coronavirus disease 2019 (COVID-19) pathogenic agent SARS-CoV-2 [1]. SARS-CoV-2 is an emerging coronavirus that originated in China in late 2019, leading to the severe illness that was recognized as COVID-19. SARS-CoV-2, similar to the previously occurred highly pathogenic human coronaviruses known as SARS-CoV, the causative agent of severe acute respiratory syndrome (SARS), has a zoonotic origin; however, the exact chain of animal-to-human transmission for SARS-CoV-2 remains unclear [2]. SARS-CoV-2 possesses a (+) ssRNA genome that aligns with the typical gene array characteristic of coronaviruses associated with the pandemic virus. It possesses one of the largest RNA genomes, approximately 30

kilobases in length, and is liable for the encoding of around 29 proteins [3]. The genomic RNA of SARS-CoV-2 has two open reading frames (ORFs). These are referred to as ORF1a and ORF1b. The ORF1a and ORF1b encode for structural protein (SP) and non-structural protein (NSP), respectively, and are found at the 5′ terminal. Meanwhile, the 3′ terminal encodes for of SPs, such as Envelope (E), Membrane (M), Nucleocapsid (N), and the Spike protein (S) [4]. Nonetheless, only a few vital virion proteins, such as S as SP and main protease (Mpro) as NSP, have been carefully investigated as potential drug binding targets for therapeutic prospects [5-9]. Whole genome sequencing (WGS) has shown its significance in tracking the genetic evolution of SARS-CoV-2 and detecting novel variants. WGS facilitates the identification of mutations across the whole viral genome, especially in crucial structural proteins such as S, M, and E, which may influence viral transmission and immune evasion. Alongside WGS, methods like Pangolin (Phylogenetic Assignment of Named Global Outbreak Lineages) are extensively used to categorize SARS-CoV-2 lineages via the examination of mutation patterns in viral genomes [10, 11]. GISAID6 and Nextstrain enabled the sharing of global data and the tracking of variants in real-time, thereby supporting timely surveillance efforts [12, 13]. The S protein of the virus interacts with human host receptors, whereas the highly conserved N, which exhibits substantial immunogenicity, is crucial for both diagnostic and therapeutic research. Meanwhile, the receptor-binding domain (RBD) of the S protein facilitates viral entry into host cells primarily by interacting with the host angiotensin-converting enzyme 2 (ACE-2) receptor. Furthermore, Mpro, a well-known SARS-CoV-2 enzyme, has been intensively studied as a plausible alternative for drug candidate affinity/binding without close human homologs [14-22]. At eleven

conserved cleavage sites, Mpro activates the viral replicase and degrades replicase polyproteins, completing the virus cycle. Protein functional and structural properties are critical for binding a diverse variety of pharmacologically active chemicals as ligands in the search for a viable therapeutic solution to address the associated illness. The continuous evolution of structural proteins hampers the determination of binding affinities for both novel and existing antiviral drugs targeting these proteins [22-24]. From the onset of the COVID-19 pandemic and the progression of the SARS-CoV-2 virus, the World Health Organization (WHO) has identified several COVID-19 Variants of Concern (VOCs) and Variants of Interest (VOIs). These designations are based on their potential to spread, replace earlier variants, trigger new waves of infection, and necessitate changes in public health strategies. The continuous mutations of SARS-CoV-2 give rise to new VOCs, which pose a heightened public health risk compared to earlier strains. VOCs represent elevated transmissibility and the ability to escape treatments, tests, and vaccines [25-27]. Among the identified VOCs, Alpha (B.1.1.7), Beta (B.1.351), Gamma (P.1), Kappa (B.1.617.1), Delta (B.1.617.2), and Omicron (B.1.1.529) are notable variants that have had a global public health impact [26-34]. In this regard, the BA.1 lineage has been reported to possess 60 mutations, of which up to 38 occur in the S protein, one in the E protein, two in the M protein, and six in the N protein [35]. Comparably, the BA.2 lineage has 57 mutations, 31 of which are in the S protein, and its N-terminus varies significantly from that of BA.1. lineage [35]. The RBD of the S protein binds to the host receptor ACE2, perhaps enhancing infectivity and facilitating evasion of vaccine-induced neutralizing antibodies as a result of mutation [35]. As a result, mutations in the RBD of the S protein have sparked attention to target this for

significant research. Alterations in the N-terminal domain (NTD) can facilitate immune evasion by the virus, while changes in the S2 region may optimize the fusion process and entry into cells [36]. Mutations in the S protein of Omicron may significantly hinder antibody-mediated neutralization and elevate the likelihood of reinfections, thereby raising significant concerns [37, 38]. In this perspective, mutations and structural changes in the S protein may contribute to an additional issue beyond the previous problem. Structural investigations of S proteins from VOCs and targeting their RBD for different antiviral drugs and mAb binding screening might assist in expanding the current understanding to cope with associated challenges. Drug discovery is a scientifically challenging, long-lasting, and costly process. Exiting antiviral drugs might be re-purposed to target RBD of S protein inhibition. The presented study investigates the structural analyses of VOCs, the binding efficiency of selected drugs and mAb to the RBD of Omicron and nCoV. The protein-protein interactions between RBD, ACE2, and mAb were investigated to comprehend the molecular interactions by comparing with the WT reference variant. However, computational findings necessitate validation through *in vitro* and further appropriate experimental assays to translate them into therapeutic applications.

2. Methods

2.1 Selection of antiviral agents against RBD

Several antiviral agents have been repurposed for the treatment of COVID-19. In line with the published scientific literature, a set of eight antiviral drugs and two mAbs were selected to be deployed in binding analyses and protein-protein interactions (mAb). Such selected antiviral agents: Remdesivir, Atazanavir, Indinavir, Lopinavir,

Favipiravir, and Molnupiravir, Oseltamivir, and Ribavirin, along with two antibodies, B38 and CA521, were included in the present study [39-48]. Two-dimensional structures in 2D coordinates in SDF format (antiviral drugs) were retrieved from the PubChem database (https://pubchem.ncbi.nlm.nih.gov), while mAb protein structures were obtained from the Protein Data Bank (PDB) (https://www.rcsb.org) [49-53]. Ligands (Table 1) were prepared and adjusted to human physiological pH, followed by structure optimization and refinement for geometric accuracy using the mmff94 algorithm in Avogadro tool (Version 1.2.0) [54, 55]. Likewise protein structure of antibodies was also optimized by removing other existing components.

2.2 Extraction and structural preparation of RBD and ACE2

Mutations in the nCoV have led to the emergence of new VOCs. A protein coordinates file (PDB) of the S protein in PDB format was deployed for structural analyses including; nCoV (PDB: 6VSB), Alpha (PDB: 7LWV), Beta (PDB: 7LYO), Gamma (PDB: 7V78), Kappa (PDB: 7V7E), Delta (PDB: 7V7Q), and Omicron (PDB: 7T9K) by retrieving from the Protein Databank (https://www.rcsb.org) [49, 56-61]. Additionally, only nCoV and Omicron variants' PDB files were prepared for binding with selected antiviral drugs with the RBD by trimming other amino acid residues, and keeping only the RBD region. This optimized portion was subsequently utilized in docking. The crystal structure of ACE2 was obtained using PDB 7C8D for the Protein-Protein docking [62, 63]. The ACE2 region was extracted from PDB 7C8D by removing unneeded fused protein structures [62]. Additionally, the structures of all proteins were analyzed to confirm the absence of water molecules in their coordinate files, alongside the correction of the missing residues.

2.3 Computational structural analyses

Structural analyses to understand the architecture of S proteins of SARS-CoV-2 VOCs were conducted by examining their constituent amino acid residues in cartoon representation by comparing all. All associated PDBs of S proteins were utilized for structural overlay through the Needleman-Wunsch algorithm, employing the BLOSUM62 matrix with a cutoff distance of 2.Å [64].

2.4 Secondary structure prediction and analyses

Proteins are essentially described by their secondary structures (SS), which include helices, turns, sheets, coils, and more, and were investigated for SARS-CoV-2 VOCs utilizing the SOPMA method (https://npsa.lyon.inserm.fr/cgi-bin/npsa_automat.pl?page=/NPSA/npsa_sopma.html). In SS prediction, the number of conformational states was set up to 4 (helix, turn, sheet, coil); the similarity threshold was set at 8; and the window width was set to be 17. After providing input data in FASTA sequence, it was subsequently computed by configuration parameters, followed by the results output.

2.5 Structural domain prediction among S proteins of VOCs

In a protein, domains represent unique functional and/or structural elements. They are usually designated for a particular function or interaction, and they play a crucial role in a protein's function by executing that function or interaction. Domains can be identified across various biological contexts, with similar domains present in proteins that serve different functions. The InterPro database from EMBL-EBI (https://www.ebi.ac.uk/interpro/) was used to predict structural domains in SARS-

CoV-2 VOCs [65, 66]. InterPro offers a functional analysis of proteins by categorizing them into families and predicting domains and significant sites [67]. InterPro facilitated the ability to get to the NTD, RBD, and S1/S2 regions in all variants of SARS-CoV-2.

2.6 Binding affinity assessment of selected drugs by employing docking

Docking was performed in GUI mode to dock selected drug compounds to the RBD of Omicron and the reference protein (RBD of nCoV) using the PyRx software (v. 0.8), which is coupled with AutoDock Vina. A grid box of 44.72 × 53.56 × 93.25 Å (X, Y, Z coordinates) was utilized to designate the 3D search area on the prepared proteins where the ligands are expected to bind. Vina exhibits that the highest-ranking binding free energy consistently has a 0 RMSD. The lowest binding free energy ranked value was taken into account as the same as 0 RMSD values. The bound protein-ligand complexes were critically analyzed for potential hydrogen bond interactions with corresponding key amino acid residues, utilizing UCSF Chimera X and the Discovery Studio visualizer (v 16.1.0.15350) software [64, 68].

2.7 Protein-protein docking analyses for exploration of RBD-ACE2, RBD- mAbs interaction

Protein-protein docking determines the optimal orientation (binding pose) of two interacting molecules by enhancing steric and physicochemical complementarity to its optimum extent. To conduct the Protein–protein docking of Omicron-ACE 2, nCoV-ACE 2, Omicron-RBD-B38, nCoV-B38, Omicron-RBD-CA521, and nCoV-CA521, the ClusPro 2.0 server (https://cluspro.bu.edu/publications.php) was utilized

for the analysis [69]. The server executes three computational operations in the following order: (1) rigid-body docking by sampling billions of conformations, (2) root-mean-square deviation (RMSD) based clustering of the 1000 lowest energy structures generated to identify the largest clusters that will represent the most likely models of the complex, and (3) refinement of selected structures using energy minimization [69]. The ClusPro free docking protocol comprises two primary phases [70]. The first step is to run PIPER, a docking tool that uses the fast Fourier transform (FFT) correlation approach to seek complicated conformations on a grid [71]. Desolvation contributions are estimated using a structure-based pairwise potential together with the van der Waals interaction energy and an electrostatic energy component. Secondly, ClusPro uses the pairwise RMSD as a distance metric to cluster the top 1000 structures created by PIPER. The Coefficient Weights of docked proteins were calculated with the following equation:

$$E=0.40E_{rep}+-0.40E_{att}+600E_{elec}+1.00E_{DARS}$$

3 Results

3.1 Computational structural analyses

Three-dimensional structures of the S proteins of SARS-CoV-2 VOCs were predicted to evaluate structural similarities by residue-to-residue alignment by superimposing each S protein. PDB data for each variant, including nCoV (6VSB), Alpha (7LWV), Beta (7LYO), Gamma (7V78), Kappa (7V7E), Delta (7V7Q), and Omicron (7T9K), were utilized for structural prediction and analysis in a single unit refined structure in cartoon without any existing ligand. Figure 1 illustrates the structural superimposition

of the S protein of VOCs, while the RBD of Omicron and nCoV, with a distance cutoff value of 2 Å RMSD, is rendered in Figure 2. An overlay-generated picture clearly shows minor color-coded changes in protein secondary structure.

3.2 Secondary structure prediction and analyses

SSE of VOCs in helix, sheet, turn, and coil configurations was predicted by implementing the SOPMA method. Significant changes can be seen in all of the SS results. The Beta (B.1.351) type possessed the lowest percentage of Alpha helix (Hh) at 26.79%, while Omicron possessed the highest percentage at 29.43%. Extended strands were found to be between 21.64% and 22.37% for all VOCs. The beta-turn was observed in all VOCs within a range of 3.54 % to -5.12 %. The random coil was observed to be within the range of 45-46.84 %. Table 2 provides a comprehensive set of results of the predicted SS results. Comparative SSE plot of S proteins of VOCs is portrayed in Figure 3.

3.3 Structural domain prediction among S proteins of VOCs

Finding and predicting specific protein structural regions is a crucial aspect of figuring out protein structure and function. Protein motifs and domains represent unique, functional evolutionary units that can be acquired, lost, or rearranged collectively as a single module more readily than other protein elements. Rapid protein construction by combining existing functional modules is enabled by this evolutionary flexibility, which contributes to protein diversity and the evolution of new functions. InterPro conducts functional analysis on proteins by dividing them into families and predicting domains and key locations based on a given protein

sequence. Structural domains from all S proteins of VOCs were predicted to encompass the variable region of amino acid residues. The predicted domain in the S protein among all VOCs is listed in Table 3. Residues-residues structural comparison of Omicron and nCoV S protein has been depicted in Figure 4.

3.4 Binding affinity assessment of selected drugs by employing docking

Molecular docking stands out as a reliable computational method for exploring the interactions of receptor-ligand binding. This step is crucial for pre-screening or virtual screening in the drug discovery and development process, as well as in repurposing efforts. Hydrogen bonding and active site residues, including the lowest binding energy with the lowest RMSD, are essential components of docking for drug-ligand docking evaluation assessment. A collection of eight drug candidates was docked with RBD (Omicron), and the results were compared to the nCoV (wild type) variant to evaluate the binding ability with corresponding ligands (Drugs). The RBD-Indinavir complex of Omicron (7T9K) seems to have the lowest binding with a binding affinity value of -7.4 ±0.06 (Kcal/mol), involving H-Bond interactions with ARG-355, ASP-428, THR-430, SER-514, and GLU-516 residues. Similarly, with a binding affinity value of -8.8±0.55 (Kcal/mol), the RBD-Lopinavir complex of nCoV (6VSB) seems to have the lowest binding affinity, which is comparatively better than omicron's top-ranked molecule, entails H-bonding with ALA-27 and ALA-143 residues. RBD of nCoV exhibited good binding affinity in a range of -5.7±0.64 to -8.8±0.55 Kcal/mol, in contrast to Omicron, which showed binding affinity in a range of -5.2 ±0.26 to -7.4 ±0.06 Kcal/mol. Residues PRO-330, ASN-331, THR-333, ASN-334, GLU-340, ARG-346, ASN-354, ARG-355, ASN-360, VAL-362, SER-99, ASP-428, THR-430, ARG-

454, ARG-457, SER-459, GLU-471, SER-494, SER-496, ARG-498, TYR-501, SER-514, GLU-516, LEU-517, CYS-525, and LYS-528 were found to be involved as common active site amino acids involved in H-bond interaction. Figure 5-6 depicts the protein-ligand interaction of Omicron and nCoV RBD in 2D. Table 4 reveals the docking assessment result in comprehensive detail. Figure 7 depicts a comparison binding affinity plot of Omicron-ligands and nCoV-ligands.

3.5 Protein-protein docking analyses for exploration of RBD-ACE2, RBD- mAbs interaction

Protein-protein docking is crucial for examining Protein-protein interactions and emphasizing interactional functionalities. The Omicron RBD-ACE2, Omicron-RBD-B38, and Omicron-RBD-CA521 combination were docked to understand the underlying binding interactions and energy scores. The protein-protein docking was compared to the nCoV variant as a reference to investigate the in-depth interaction attributes and comprehend Omicron binding against antibodies and the ACE2 receptor. The Omicron-ACE2 docked complex demonstrated a score of -846.2 (center) and -846.2 (Lowest Energy) for the 0 cluster, which is significantly better than the reference docked complex (nCoV-ACE2), which had a score of -648.6 (center) and -703.1 (Lowest Energy). Omicron- B38 (Antibody) protein-protein docking scores exhibited -728.0 (Center), -873.7 (Lowest Energy) scores for 0 clusters. Score values of this Protein-protein complex were not comparable or had minor fluctuating values with reference docked complex (nCoV-B38), which seems to have score values of -706.8 (center), and -924.0 (Lowest Energy), respectively. Omicron-CA521 (Antibody) docked complex exhibited score values as -836.6

(center), -930.7 (Lowest Energy), respectively, for 0 clusters. Comparatively, this score was better than the reference docked complex (nCoV-CA521), which exhibited score values of -139.4 (Center), -162.6 (Lowest Energy), respectively. Selected docked protein-protein complexes are highlighted in Figures 8-9. The findings of Protein-mAb (Omicron-Antibodies) and Protein-ACE2 suggested a significantly better binding behavior than the reference complexes. Table 5 lists the comprehensive results of the protein-protein docking.

4. Discussion

SARS-CoV-2, the infectious agent that causes COVID-19, was prone to mutations and the rise of genetic variations that emerge as VOCs. Since its initial emergence in 2019, SARS-CoV-2 has undergone continuous evolution, leading to the emergence of various lineages and VOCs that exhibit enhanced transmission efficiency, increased severity, and improved immune evasion capabilities. The WHO has designated these variants using nomenclature derived from the Greek Alphabet, starting with the Alpha (B.1.1.7) variant, which surfaced in 2020, succeeded by the Beta (B.1.351), Gamma (P.1), Delta (B.1.617.2), and Omicron (B.1.1.529) variants [72]. Each VOC has a unique mutation in the S protein, which influences pathogenicity, transmissibility, and evasion of diagnostic tests and vaccination [73, 74]. Among the various VOCs, the Omicron variant stands out as the most genetically diverse, having evolved into multiple distinct sub-lineages that the WHO has classified as VOIs. BA.1, BA.1.1, BA.2, BA.2.12.1, BA.2.13, BA.2.38, BA.2.75, BA.3, BA.4, and BA.5 [72]. BA.4 and BA.5 continue to be the most prevalent and notable variants, while some novel sub variants, such as BA.2.75.2 (B.F 7), BA.4.6,

BA.4.7, BA.5.9, BF.7, BQ.1, BQ.1.1, BN.1, XBB, XBB 1.5, XBB 1.6, and CH.1.1, have emerged from various previously circulating sub-lineages of Omicron worldwide [72]. Nevertheless, a variety of medicines, including antiviral agents and a few additional antibiotics, have shown efficacy in treating novel SARS-CoV-2-associated diseases (COVID-19) [75, 76]. Consequently, the most recent variant, Omicron, characterized by a notably high mutation rate, has resulted in a new phase in the global epidemic. Exploring the pathogenicity of novel SARS-CoV-2 variants could significantly enhance our understanding through structural and functional studies. Additionally, identifying the molecular interactions between antiviral drugs and antibodies will be crucial for addressing future outbreaks and treating diseases associated with SARS-CoV-2. In this instance, multiple monoclonal antibodies have also demonstrated effectiveness for both prevention and treatment of SARS-CoV-2 infection [77-79]. Further exploration remains challenging; therefore, this study examined the structural and functional properties of S protein variations of Omicron in relation to the binding affinity of antiviral drugs and mAb. A comprehensive evaluation was conducted on eight recognized antiviral drugs to assess their binding affinity with the RBD of the S protein of Omicron variants, with a comparative analysis against the nCoV variant to facilitate an in-depth understanding of binding affinity. Additionally, two antibodies were evaluated for their binding interactions with the RBD, highlighting the significance of the protein-protein interaction. The structure of the entire S protein of VOCs, along with the RBD of Omicron and nCoV, reveals significant differences when analyzed through structural overlay. The constituent SSE in S proteins of VOCs ranged from 3.54% to 46.84% across all categories, including Alpha helix, Extended strand, Beta turn, and Random coil. The far lowest

Alpha helix percentage was observed for nCoV as 26.86%, while the highest was noted in Omicron at 29.43%. The extended strand (Ee) was measured between 21.64 % (Omicron) and 22.37% (Gamma). The beta turn (Tt) elements were observed to be the lowest in comparison to SSE, as 3.54 % (Omicron) to 5.12% (nCoV). Random coil (Cc) element noted the highest SSE as 45.40% (Omicron) to 45.99% (Gamma). The binding affinity of the RBD with selected antiviral drugs indicates potential binding affinity with potential interaction by H-Bond with associated active site residues. Notable binding affinity observed for the RBD-Lopinavir complex of nCoV, with a lowest binding energy of -8.8±0.55 Kcal/mol, involving the residues ALA-27 and ALA-143, which were involved in H-Bond. Likewise, RBD of Omicron- Indinavir exhibited a strong binding affinity, with a value of -7.4 ±0.06 Kcal/mol. This has H-Bond interactions with ARG-355, ASP-428, THR-430, SER-514, and GLU-516 residues. The binding scores for the Omicron-ACE2 and Omicron-antibody (2 mAb) complexes indicate adequate binding energy and interaction. The Omicron RBD-ACE2 complex exhibited scores of -846.2 for the Center and -846.2 for the lowest energy, respectively. In contrast to the reference complex (nCoV RBD-ACE2), which exhibited a slightly lower score for center only as -648.6, whilst the Lowest Energy score was higher (-703.1). Omicron-RBD-B38 complex was found to have a good energy Score (Center -728.0), and a weak Lowest energy score (-873.7) than the reference complex (nCoV RBD-B38), which had -706.8 (Center), and -924.0 (Lowest Energy). Omicron-RBD-CA521 complex exhibited a protein-protein docking score value for 0 cluster as -836.6 (center), -930.7 (Lowest Energy). In contrast to nCoV-RBD-CA521, this had a better energy score. Protein-Protein docking scores support the significant binding abilities of the

RBD of Omicron to the ACE2 receptor and selected antibodies. Top-ranked docked complexes can be validated through MD simulations and subsequently by an *in vitro* experiment, which might enhance the comprehension of Omicron functionality at the molecular level. Nevertheless, additional experimental validation can be conducted to repurpose evaluated antiviral drugs for the effective management of future SARS-CoV-2-related illnesses.

5. Conclusion

The S protein mutation results in structural changes that enhance pathogenicity, increase transmissibility, and enable immune evasion in the SARS-CoV-2 variants. The mutation appeared as the key factor in the development of a highly transmissible variant of SARS-CoV-2, which was known as Omicron. A notable mutation in the RBD of Omicron has altered its binding affinity for antiviral drugs and antibodies. Such attributes were undertaken with the present study, implementing eight antiviral drugs and two mAbs. Findings on multivalent computational parameters suggested significant changes in S proteins, including RBD, and variable binding affinity among ligands and mAb. SSE exhibited a significant variation in constituent elements among VOCs. The binding affinity of RBD (Omicron) with antiviral drugs exhibited a notable binding potential in a range of -5.2 ±0.26 to -7.4 ±0.06 Kcal/mol. Likewise, Protein-Protein docking further elucidated the binding dynamics between the Omicron-ACE2 receptor and selected mAb. The computational findings of selected drugs and mAb exhibited a significant binding capacity, which could be further extended by implementing MD simulation and

experimental validation, which might be helpful for further investigation to understand the efficacy of antiviral drugs against the RBD of mutant and future sub-variants.

List of Abbreviations:

Angiotensin-Converting Enzyme 2 (ACE-2)

Coronavirus Disease 2019 (COVID-19)

Fast Fourier Transform (FFT)

N-terminal Domain (NTD)

Non-Structural Protein (NSP)

Open Reading Frames (ORFs)

Receptor-Binding Domain (RBD)

Root-Mean-Square Deviation (RMSD)

Secondary Structural Element (SSE)

Severe Acute Respiratory Syndrome (SARS)

Structural Protein (SP)

Variant of Concern (VOC)

Variants of Interest (VOIs)

Whole genome sequencing (WGS)

Author contributions

SKK: Conceptualization, Data curation, Formal analysis, Investigation, Methodology, Validation, Software, Writing–original draft, Writing – review & editing, and Supervision. **KHV:** Data curation, Formal analysis, Investigation, Methodology, Validation, Software, Writing – review & editing. **AKS:** Conceptualization, Data

curation, Formal analysis, Investigation, Methodology, Validation, Software, Project administration, Writing–original draft, Writing – review & editing, visualization and Supervision. All authors have read and approved the published version of the manuscript.

Availability of data and materials

All data used in the present study were generated from computational experiments and are provided in the present study. Data associated with the results are available upon request from the corresponding authors.

Conflicts of interest

Authors have no actual or potential conflicts of interest, including any financial, personal, or other relationships with other people or organizations that could inappropriately influence, or be perceived to influence their work.

Funding:

No funding was available to support this study.

Acknowledgment

SKK is highly thankful to VFSTR (Deemed to be University) for providing the faculty seed grant (F.No. VFSTR/REG/A6/30/2023-24/01 dated 16-05-2023). AKS thankfully acknowledges the “Academy of Scientific and Innovative Research (AcSIR)”, Ghaziabad, India (An *Institute of National Importance).*

AI-declaration:

No AI-generated text, figures, or data have been used in this research manuscript; all are original content of the authors generated by experimental data.

References

1. Pal, M., et al., *Severe Acute Respiratory Syndrome Coronavirus-2 (SARS-CoV-2): An Update.* Cureus, 2020. **12**(3): p. e7423-e7423.
2. Pagani, I., et al., *Origin and evolution of SARS-CoV-2.* The European Physical Journal Plus, 2023. **138**(2): p. 157.
3. Cao, C., et al., *The architecture of the SARS-CoV-2 RNA genome inside virion.* Nature Communications, 2021. **12**(1): p. 3917.
4. Mariano, G., et al., *Structural Characterization of SARS-CoV-2: Where We Are, and Where We Need to Be.* Frontiers in Molecular Biosciences, 2020. **Volume 7 - 2020**.
5. Suárez, D. and N. Díaz, *SARS-CoV-2 Main Protease: A Molecular Dynamics Study.* Journal of Chemical Information and Modeling, 2020. **60**(12): p. 5815-5831.
6. Bojadzic, D., et al., *Small-Molecule Inhibitors of the Coronavirus Spike: ACE2 Protein-Protein Interaction as Blockers of Viral Attachment and Entry for SARS-CoV-2.* ACS Infect Dis, 2021. **7**(6): p. 1519-1534.
7. Unni, S., et al., *Identification of a repurposed drug as an inhibitor of Spike protein of human coronavirus SARS-CoV-2 by computational methods.* J Biosci, 2020. **45**(1).

8. Xia, S., et al., *Inhibition of SARS-CoV-2 (previously 2019-nCoV) infection by a highly potent pan-coronavirus fusion inhibitor targeting its spike protein that harbors a high capacity to mediate membrane fusion.* Cell Research, 2020. **30**(4): p. 343-355.

9. Goc, A., et al., *Phenolic compounds disrupt spike-mediated receptor-binding and entry of SARS-CoV-2 pseudo-virions.* PLOS ONE, 2021. **16**(6): p. e0253489.

10. O'Toole, Á., et al., *Assignment of epidemiological lineages in an emerging pandemic using the pangolin tool.* Virus Evolution, 2021. **7**(2): p. veab064.

11. Rambaut, A., et al., *A dynamic nomenclature proposal for SARS-CoV-2 lineages to assist genomic epidemiology.* Nature Microbiology, 2020. **5**(11): p. 1403-1407.

12. Shu, Y. and J. McCauley, *GISAID: Global initiative on sharing all influenza data–from vision to reality.* Eurosurveillance, 2017. **22**(13): p. 30494.

13. Hadfield, J., et al., *Nextstrain: real-time tracking of pathogen evolution.* Bioinformatics, 2018. **34**(23): p. 4121-4123.

14. Gajjar, N.D., T.M. Dhameliya, and G.B. Shah, *In search of RdRp and Mpro inhibitors against SARS CoV-2: Molecular docking, molecular dynamic simulations and ADMET analysis.* J Mol Struct, 2021. **1239**: p. 130488.

15. Qiao, J., et al., *SARS-CoV-2 M(pro) inhibitors with antiviral activity in a transgenic mouse model.* Science, 2021. **371**(6536): p. 1374-1378.

16. Vuong, W., et al., *Improved SARS-CoV-2 Mpro inhibitors based on feline antiviral drug GC376: Structural enhancements, increased solubility, and*

micellar studies. European Journal of Medicinal Chemistry, 2021. **222**: p. 113584.

17. Gossen, J., et al., *A Blueprint for High Affinity SARS-CoV-2 Mpro Inhibitors from Activity-Based Compound Library Screening Guided by Analysis of Protein Dynamics.* ACS Pharmacology & Translational Science, 2021. **4**(3): p. 1079-1095.
18. Ghahremanpour, M.M., et al., *Identification of 14 Known Drugs as Inhibitors of the Main Protease of SARS-CoV-2.* ACS Medicinal Chemistry Letters, 2020. **11**(12): p. 2526-2533.
19. Jin, Z., et al., *Structure of Mpro from SARS-CoV-2 and discovery of its inhibitors.* Nature, 2020. **582**(7811): p. 289-293.
20. Rut, W., et al., *SARS-CoV-2 Mpro inhibitors and activity-based probes for patient-sample imaging.* Nature Chemical Biology, 2021. **17**(2): p. 222-228.
21. Agrawal, P.K., C. Agrawal, and G. Blunden, *Rutin: A Potential Antiviral for Repurposing as a SARS-CoV-2 Main Protease (Mpro) Inhibitor.* Natural Product Communications, 2021. **16**(4): p. 1934578X21991723.
22. Jeffery-Smith, A., et al., *Reinfection with new variants of SARS-CoV-2 after natural infection: a prospective observational cohort in 13 care homes in England.* The Lancet Healthy Longevity, 2021. **2**(12): p. e811-e819.
23. Harvey, W.T., et al., *SARS-CoV-2 variants, spike mutations and immune escape.* Nature Reviews Microbiology, 2021. **19**(7): p. 409-424.
24. Pan, H., et al., *Repurposed Antiviral Drugs for Covid-19 - Interim WHO Solidarity Trial Results.* N Engl J Med, 2021. **384**(6): p. 497-511.

25. Sheikh, A., et al., *SARS-CoV-2 Delta VOC in Scotland: demographics, risk of hospital admission, and vaccine effectiveness.* The Lancet, 2021. **397**(10293): p. 2461-2462.

26. Karim, S.S.A. and Q.A. Karim, *Omicron SARS-CoV-2 variant: a new chapter in the COVID-19 pandemic.* The Lancet, 2021. **398**(10317): p. 2126-2128.

27. Dejnirattisai, W., et al., *Reduced neutralisation of SARS-CoV-2 omicron B.1.1.529 variant by post-immunisation serum.* The Lancet.

28. WHO: Tracking SARS-CoV-2 variants (VOC), https://www.who.int/en/activities/tracking-SARS-CoV-2-variants/. (Accessed: 25 February 2026).

29. Nonaka, C.K.V., et al., *SARS-CoV-2 variant of concern P.1 (Gamma) infection in young and middle-aged patients admitted to the intensive care units of a single hospital in Salvador, Northeast Brazil, February 2021.* International Journal of Infectious Diseases, 2021. **111**: p. 47-54.

30. Slavov, S.N., et al., *Genomic monitoring unveil the early detection of the SARS-CoV-2 B.1.351 (beta) variant (20H/501Y.V2) in Brazil.* J Med Virol, 2021. **93**(12): p. 6782-6787.

31. Chemaitelly, H., R. Bertollini, and L.J. Abu-Raddad, *Efficacy of Natural Immunity against SARS-CoV-2 Reinfection with the Beta Variant.* New England Journal of Medicine, 2021.

32. da Silva, J.F., et al., *Cluster of SARS-CoV-2 Gamma Variant Infections, Parintins, Brazil, March 2021.* Emerg Infect Dis, 2022. **28**(1): p. 262-264.

33. McCallum, M., et al., *Molecular basis of immune evasion by the Delta and Kappa SARS-CoV-2 variants.* Science, 2021. **374**(6575): p. 1621-1626.

34. Grant, R., et al., *Impact of SARS-CoV-2 Delta variant on incubation, transmission settings and vaccine effectiveness: Results from a nationwide case-control study in France.* The Lancet Regional Health – Europe.

35. Fan, Y., et al., *SARS-CoV-2 Omicron variant: recent progress and future perspectives.* Signal Transduction and Targeted Therapy, 2022. **7**(1): p. 141.

36. PDB-101: Molecule of the Month, *https://pdb101.rcsb.org/motm/264*. (Accessed: 25 February 2026) (http://doi.org/10.2210/rcsb_pdb/mom_2021_12)

37. Liu, L., et al., *Striking antibody evasion manifested by the Omicron variant of SARS-CoV-2.* Nature, 2022. **602**(7898): p. 676-681.

38. Wilhelm, A., et al., *Limited neutralisation of the SARS-CoV-2 Omicron subvariants BA.1 and BA.2 by convalescent and vaccine serum and monoclonal antibodies.* eBioMedicine, 2022. **82**.

39. Wang, Y., et al., *Remdesivir in adults with severe COVID-19: a randomised, double-blind, placebo-controlled, multicentre trial.* The Lancet, 2020. **395**(10236): p. 1569-1578.

40. Kokic, G., et al., *Mechanism of SARS-CoV-2 polymerase stalling by remdesivir.* Nature Communications, 2021. **12**(1): p. 279.

41. Fintelman-Rodrigues, N., et al., *Atazanavir, Alone or in Combination with Ritonavir, Inhibits SARS-CoV-2 Replication and Proinflammatory Cytokine Production.* Antimicrob Agents Chemother, 2020. **64**(10).

42. Kalantari, S., et al., *Comparing the effectiveness of Atazanavir/Ritonavir/Dolutegravir/Hydroxychloroquine and*

Lopinavir/Ritonavir/Hydroxychloroquine treatment regimens in COVID-19 patients. Journal of Medical Virology, 2021. **93**(12): p. 6557-6565.

43. Horby, P.W., et al., *Lopinavir–ritonavir in patients admitted to hospital with COVID-19 (RECOVERY): a randomised, controlled, open-label, platform trial.* The Lancet, 2020. **396**(10259): p. 1345-1352.
44. Meini, S., et al., *Role of Lopinavir/Ritonavir in the Treatment of Covid-19: A Review of Current Evidence, Guideline Recommendations, and Perspectives.* Journal of clinical medicine, 2020. **9**(7): p. 2050.
45. Driouich, J.-S., et al., *Favipiravir antiviral efficacy against SARS-CoV-2 in a hamster model.* Nature Communications, 2021. **12**(1): p. 1735.
46. Cai, Q., et al., *Experimental Treatment with Favipiravir for COVID-19: An Open-Label Control Study.* Engineering, 2020. **6**(10): p. 1192-1198.
47. Frediansyah, A., et al., *Antivirals for COVID-19: A critical review.* Clinical Epidemiology and Global Health, 2021. **9**: p. 90-98.
48. Fischer, W.A., et al., *A phase 2a clinical trial of molnupiravir in patients with COVID-19 shows accelerated SARS-CoV-2 RNA clearance and elimination of infectious virus.* Science Translational Medicine. **14**(628): p. eabl7430.
49. Berman, H.M., et al., *The Protein Data Bank.* Nucleic acids research, 2000. **28**(1): p. 235-242.
50. RCSB Protein Data Bank (PDB); Structure 7E23, https://www.rcsb.org/structure/7E23 (Accessed: 25 February 2026). PDB DOI: https://doi.org/10.2210/pdb7E23/pdb

51. RCSB Protein Data Bank (PDB); Structure 7BZ5, https://www.rcsb.org/structure/7bz5 (Accessed: 25 February 2026). PDB DOI: https://doi.org/10.2210/pdb7BZ5/pdb

52. Wu, Y., et al., *A noncompeting pair of human neutralizing antibodies block COVID-19 virus binding to its receptor ACE2.* Science, 2020. **368**(6496): p. 1274-1278.

53. Song, D., et al., *Structure and function analysis of a potent human neutralizing antibody CA521FALA against SARS-CoV-2.* Communications Biology, 2021. **4**(1): p. 500.

54. Halgren, T.A., *MMFF VI. MMFF94s option for energy minimization studies.* Journal of Computational Chemistry, 1999. **20**(7): p. 720-729.

55. Hanwell, M.D., et al., *Avogadro: an advanced semantic chemical editor, visualization, and analysis platform.* Journal of Cheminformatics, 2012. **4**(1): p. 17.

56. RCSB Protein Data Bank (PDB); Structure 6VSB, https://www.rcsb.org/structure/6VSB (Accessed: 25 February 2026). PDB DOI: https://doi.org/10.2210/pdb6VSB/pdb

57. RCSB Protein Data Bank (PDB); Structure 7LWV, https://www.rcsb.org/structure/7lwv. (Accessed: 25 February 2026). PDB DOI: https://doi.org/10.2210/pdb7LWV/pdb

58. RCSB Protein Data Bank (PDB); Structure 7LYO, https://www.rcsb.org/structure/7lyo. (Accessed: 25 February 2026). PDB DOI: https://doi.org/10.2210/pdb7LYO/pdb

59. RCSB Protein Data Bank (PDB); Structure 7V78, https://www.rcsb.org/structure/7V78. (Accessed: 25 February 2026). PDB DOI: https://doi.org/10.2210/pdb7V78/pdb

60. RCSB Protein Data Bank (PDB); Structure 7V7E, https://www.rcsb.org/structure/7V7E. (Accessed: 25 February 2026). PDB DOI: https://doi.org/10.2210/pdb7V7E/pdb

61. RCSB Protein Data Bank (PDB); Structure 7V7Q, https://www.rcsb.org/structure/7V7Q. (Accessed: 25 February 2026). PDB DOI: https://doi.org/10.2210/pdb7V7Q/pdb

62. RCSB Protein Data Bank (PDB); Structure 7C8D, https://www.rcsb.org/structure/7C8D (Accessed: 25 February 2026). PDB PDB DOI: https://doi.org/10.2210/pdb7C8D/pdb

63. Wu, L., et al., *Broad host range of SARS-CoV-2 and the molecular basis for SARS-CoV-2 binding to cat ACE2.* Cell Discovery, 2020. **6**(1): p. 68.

64. Pettersen, E.F., et al., *UCSF ChimeraX: Structure visualization for researchers, educators, and developers.* Protein Science, 2021. **30**(1): p. 70-82.

65. Blum, M., et al., *The InterPro protein families and domains database: 20 years on.* Nucleic Acids Research, 2021. **49**(D1): p. D344-D354.

66. Apweiler, R., et al., *The InterPro database, an integrated documentation resource for protein families, domains and functional sites.* Nucleic acids research, 2001. **29**(1): p. 37-40.

67. InterPro database from EMBL-EBI, https://www.ebi.ac.uk/interpro/. (Accessed: 25 February 2026).

68. Studio, D., *BIOVIA, Dassault Systèmes, [Discovery Studio], [v 16.1.0.15350], San Diego: Dassault Systèmes, [2021].*

69. Kozakov, D., et al., *The ClusPro web server for protein-protein docking.* Nature protocols, 2017. **12**(2): p. 255-278.

70. Ghani, U., et al., *Improved Docking of Protein Models by a Combination of Alphafold2 and ClusPro.* bioRxiv, 2021: p. 2021.09.07.459290.

71. Kozakov, D., et al., *PIPER: An FFT-based protein docking program with pairwise potentials.* Proteins: Structure, Function, and Bioinformatics, 2006. **65**(2): p. 392-406.

72. Andre, M., et al. *From Alpha to Omicron: How Different Variants of Concern of the SARS-Coronavirus-2 Impacted the World*. Biology, 2023. **12**, DOI: 10.3390/biology12091267.

73. Dejnirattisai, W., et al., *Omicron-B.1.1.529 leads to widespread escape from neutralizing antibody responses.* bioRxiv, 2021: p. 2021.12.03.471045.

74. Zhang, L., et al., *The significant immune escape of pseudotyped SARS-CoV-2 variant Omicron.* Emerging Microbes & Infections, 2022. **11**(1): p. 1-5.

75. Hannan, T.B., et al., *Antibiotic usage patterns in COVID-19 patients in five tertiary hospitals from Bangladesh: A countrywide picture.* IJID Regions, 2024. **12**: p. 100381.

76. Mawazi, S.M., et al., *Antiviral therapy for COVID-19 virus: A narrative review and bibliometric analysis.* The American Journal of Emergency Medicine, 2024. **85**: p. 98-107.

77. Stadler, E., et al., *Monoclonal antibody levels and protection from COVID-19.* Nature Communications, 2023. **14**(1): p. 4545.

78. Fenwick, C., et al., *A highly potent antibody effective against SARS-CoV-2 variants of concern.* Cell Reports, 2021. **37**(2).

79. Sun, Y. and M. Ho, *Emerging antibody-based therapeutics against SARS-CoV-2 during the global pandemic.* Antibody Therapeutics, 2020. **3**(4): p. 246-256.

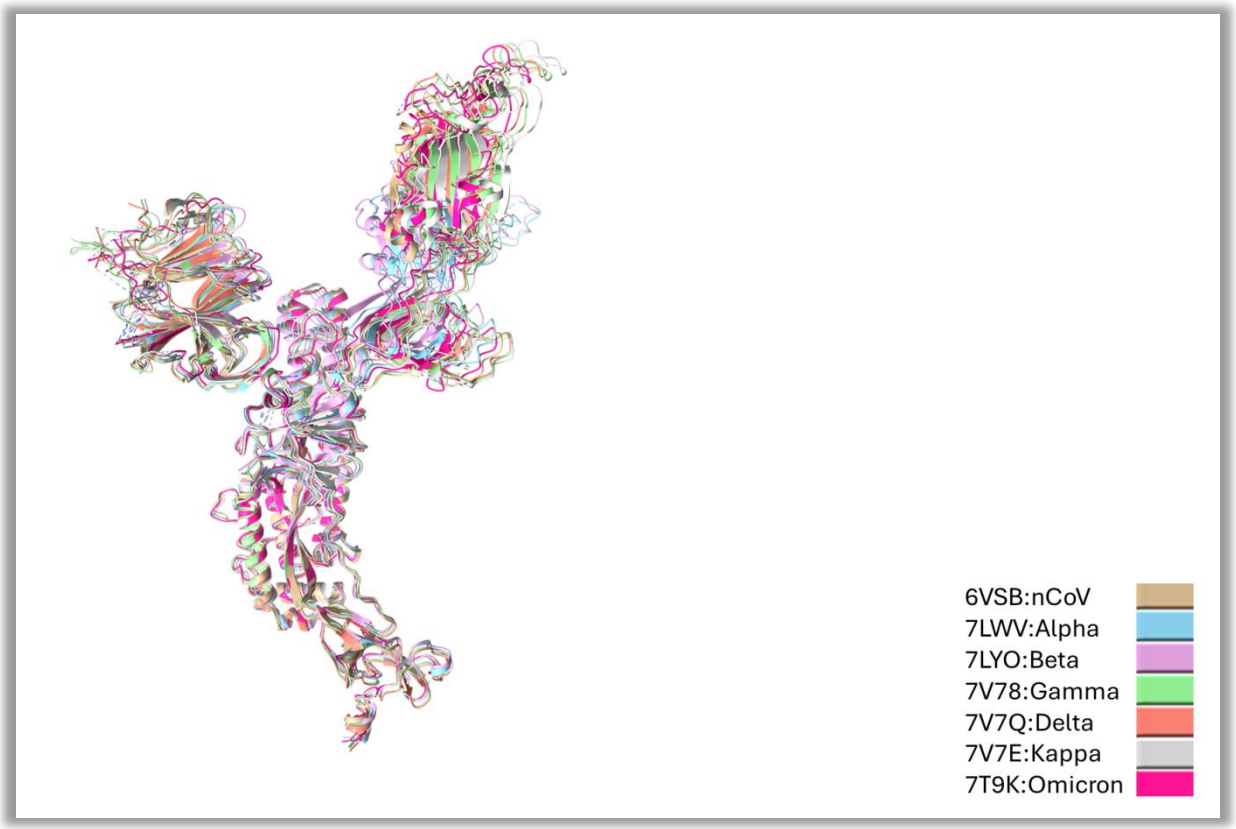

Figure 1 Structural comparison by aligning residue-residue as superimposition of the S protein of VOCs. VOCs have been marked in color code as shown in above figure.

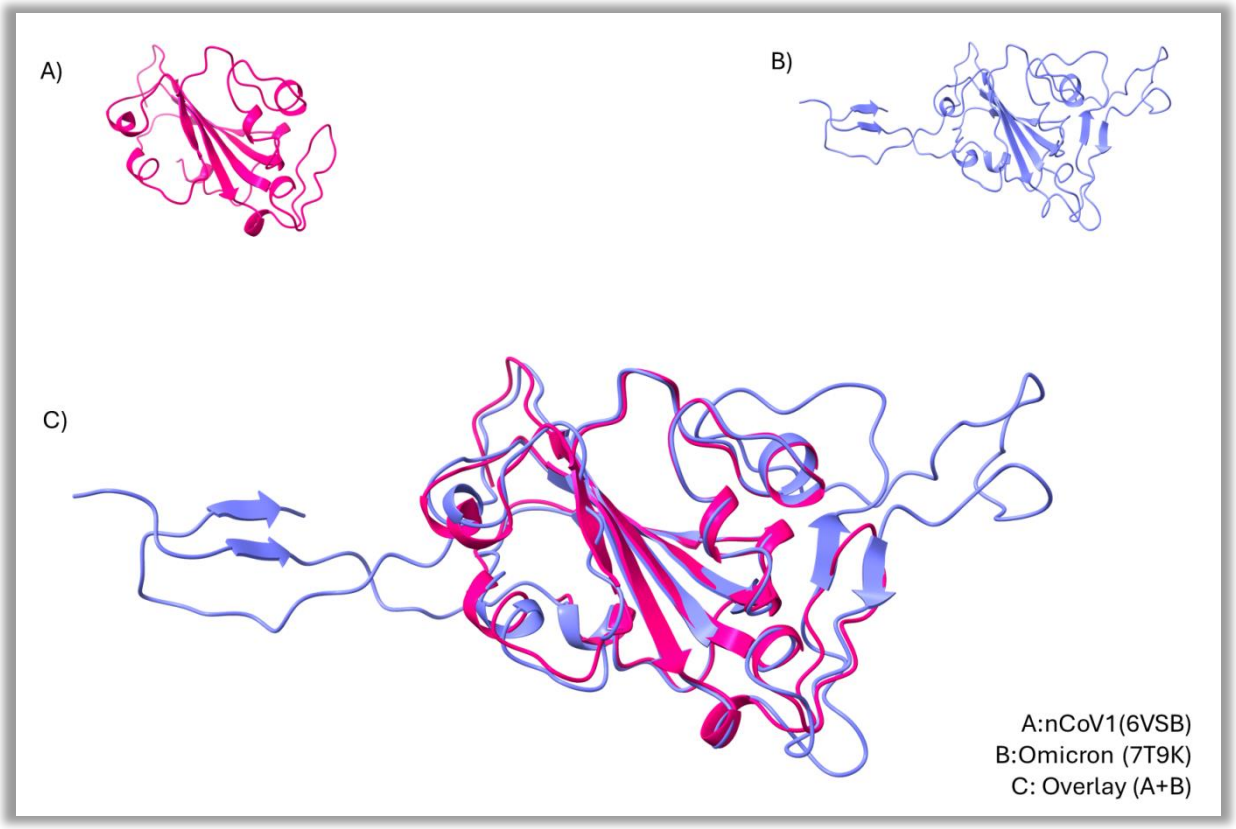
A)
B)
C)
A:nCoV1(6VSB)
B:Omicron (7T9K)
C: Overlay (A+B)

Figure 2 Structural comparison of RBD of Omicron and nCoV, with a distance cutoff value of 2 Å RMSD, in cartoon rendered. A clear change can be observed through Omicron, which has a slightly larger N-terminal and a similar C-terminal, which is extended into the left side (A): nCOV1(6vsb), (B): Omicron (7T9K), (c): Overlay (A+B).

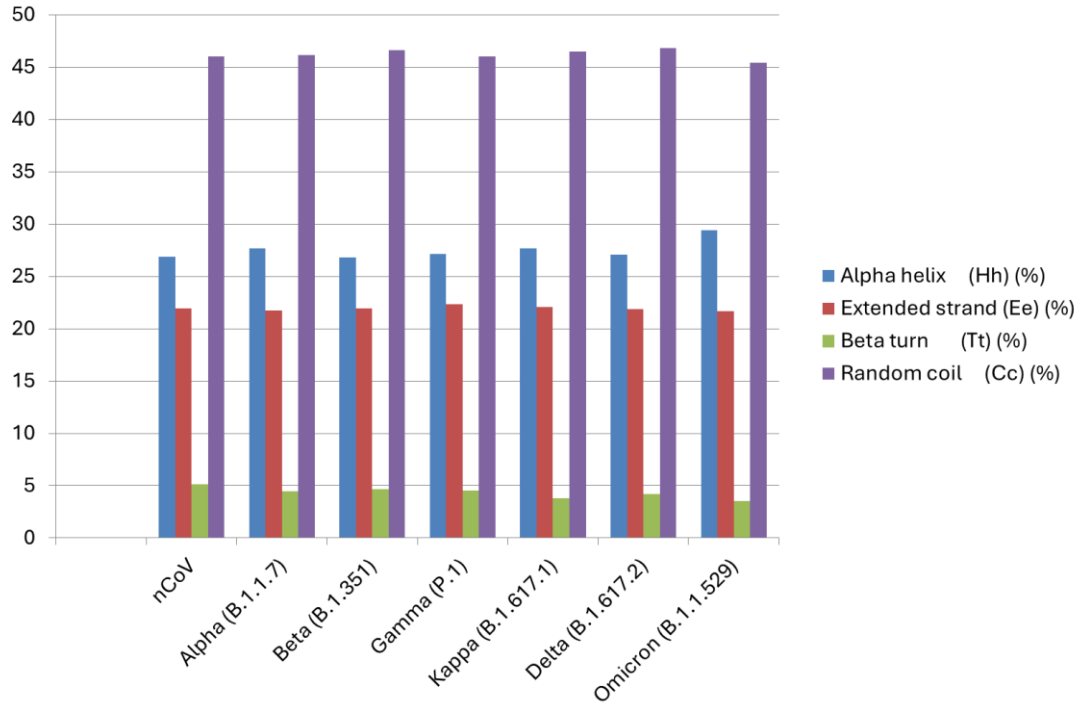

Figure 3 Comparative SSE plot of S proteins of VOCs is portrayed in percentage of elements.

2026, Vol. 3
doi:10.x/journal.x.x.x

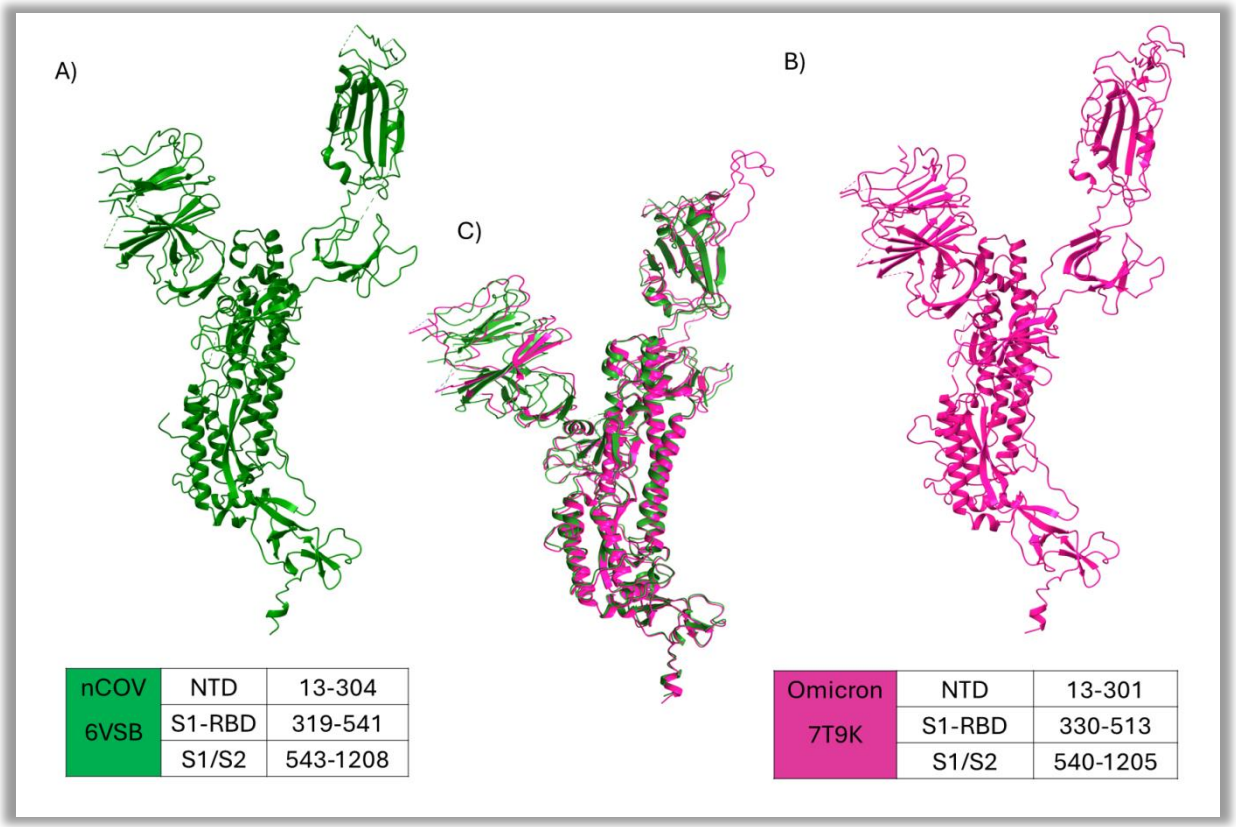

Figure 4 Structural depiction of spike protein with its structural domain details, and structural comparison. A) Represents the spike protein of nCoV (6VSB). B): represents spike protein of Omicron (7T9K). C) overlay of both structures within 2Å RMSD. The structural domain comprising NTD, S1-RBD, S1/S2 region is described in the corresponding table at bottom.

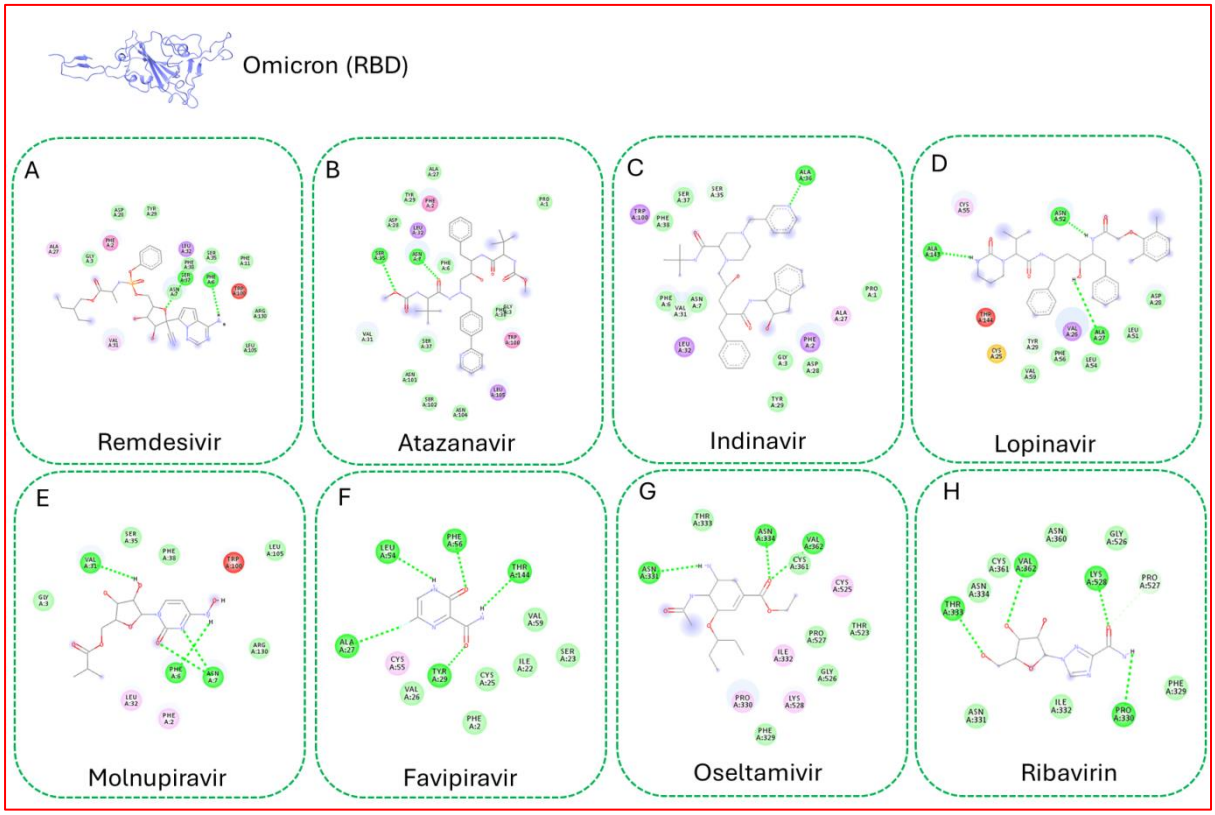

Figure 5 Docking pose of the protein-ligand interaction of Omicron with selected drugs (A) Remdesivir, (B) Atazanavir, (C) Indinavir, (D) Lopinavir, (E) Molnupiravir, (F) Favipiravir, (G) Oseltamivir, (H) Ribavirin. H-Bond among corresponding ligands is shown in 2D interaction figures.

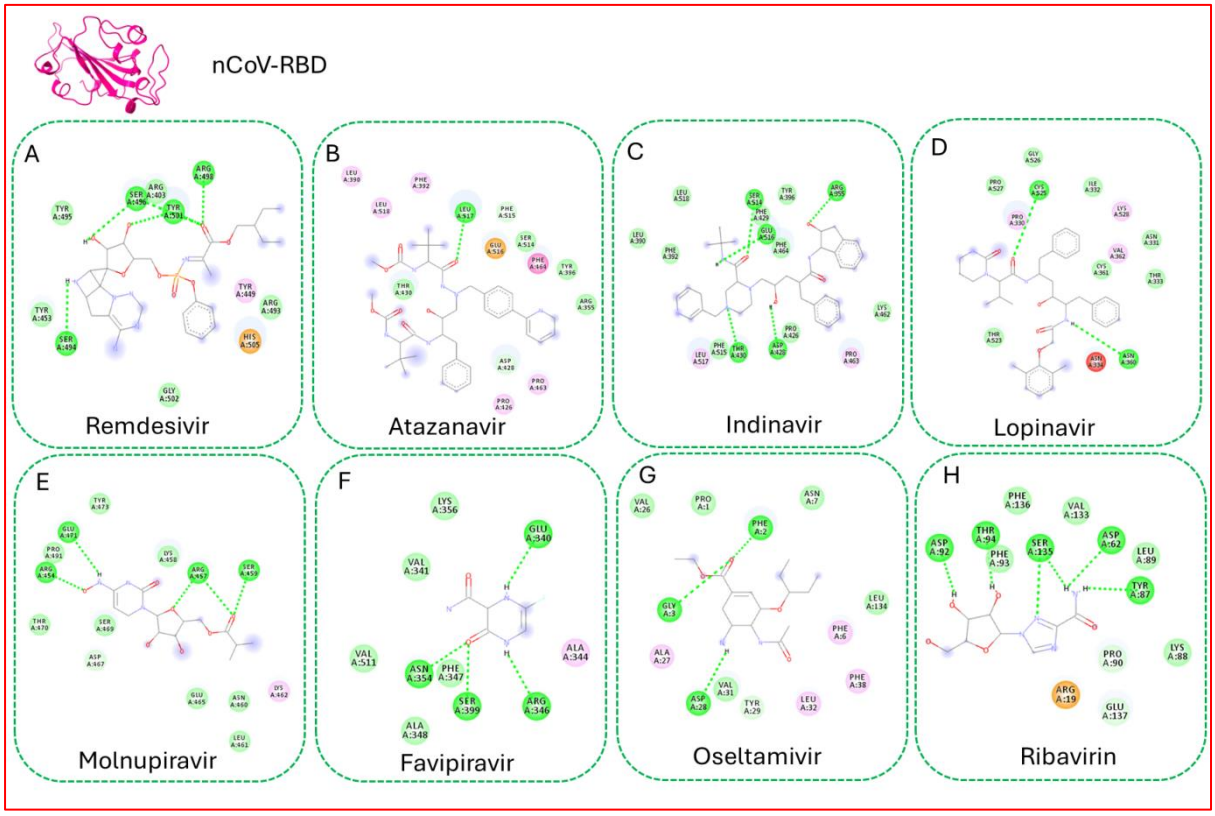

Figure 6 Docking pose of the protein-ligand interaction of nCoV with selected drugs (A) Remdesivir, (B) Atazanavir, (C) Indinavir, (D) Lopinavir, (E) Molnupiravir, (F) Favipiravir, (G) Oseltamivir, (H) Ribavirin. H-Bond among corresponding ligands is shown in 2D interaction figures.

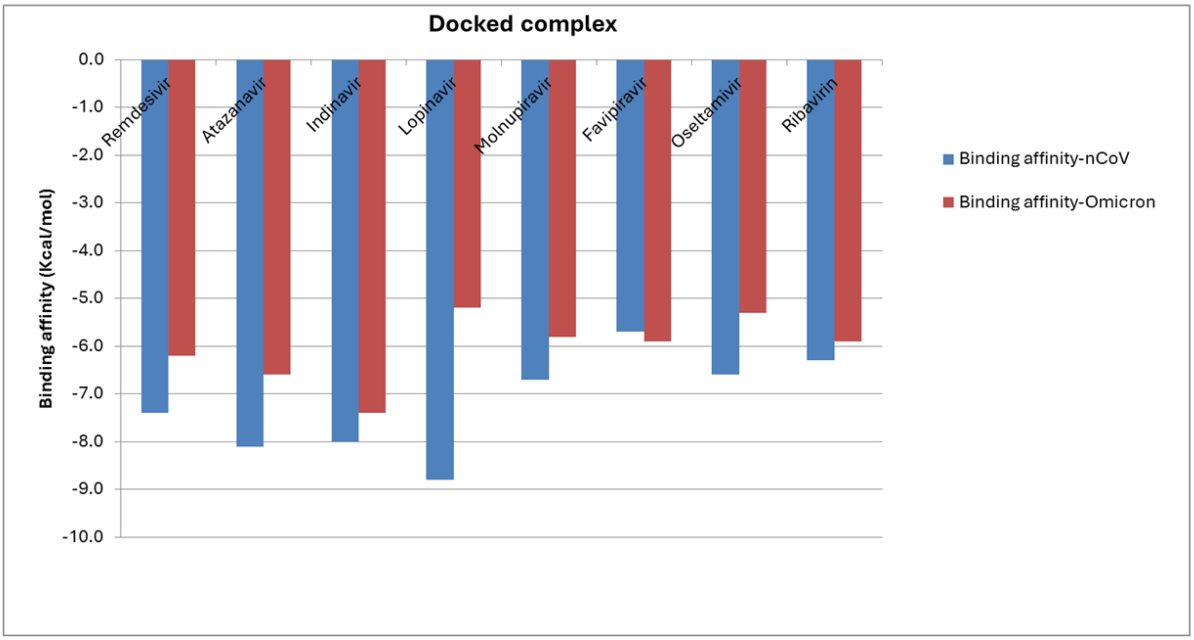

Figure 7 Highlights a comparative binding affinity plot of Omicron-ligands and nCoV-ligands docked complexes.

2026, Vol. 3
doi:10.x/journal.x.x.x

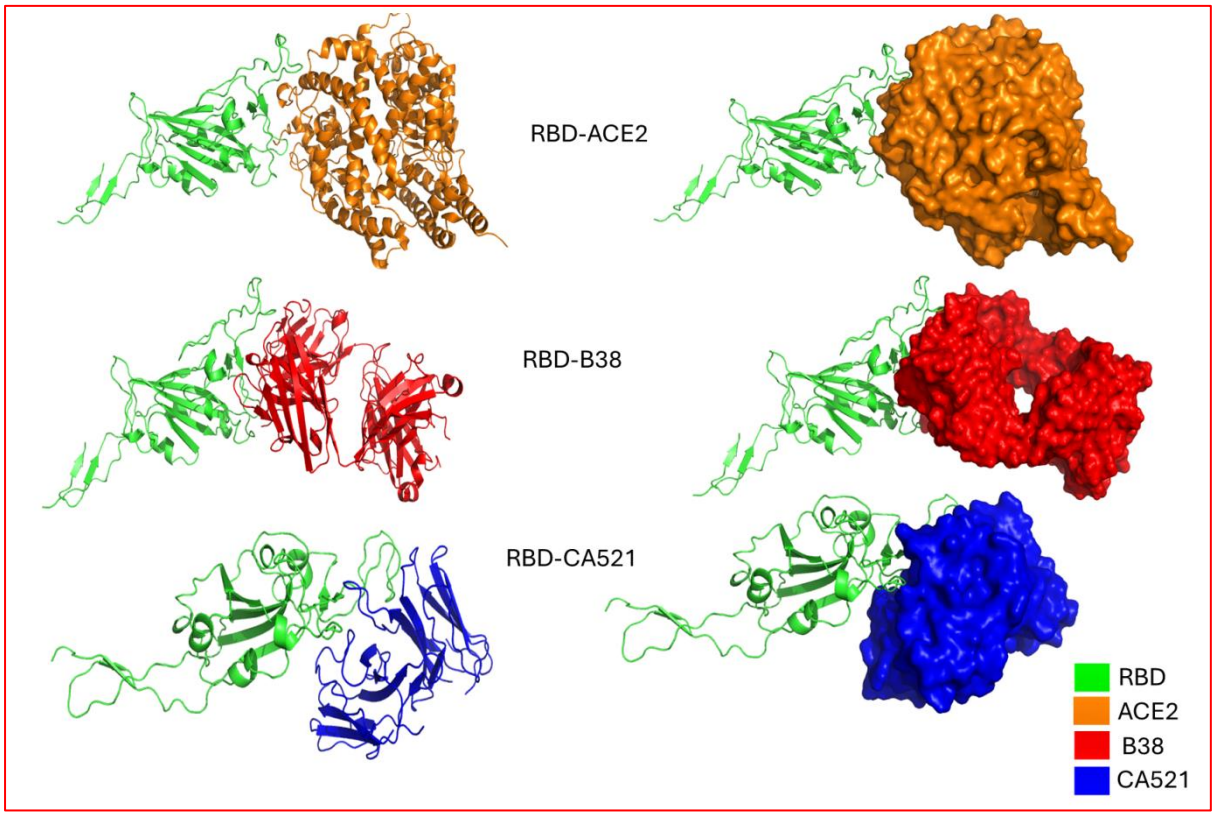

Figure 8 Protein-protein docked complexes of Omicron, with corresponding antibodies and ACE2 receptor. Color-coded keys depict the different components of docked complexes. Green: RBD; Orange: ACE2; Red: B38 antibody; Blue: CA521 antibody.

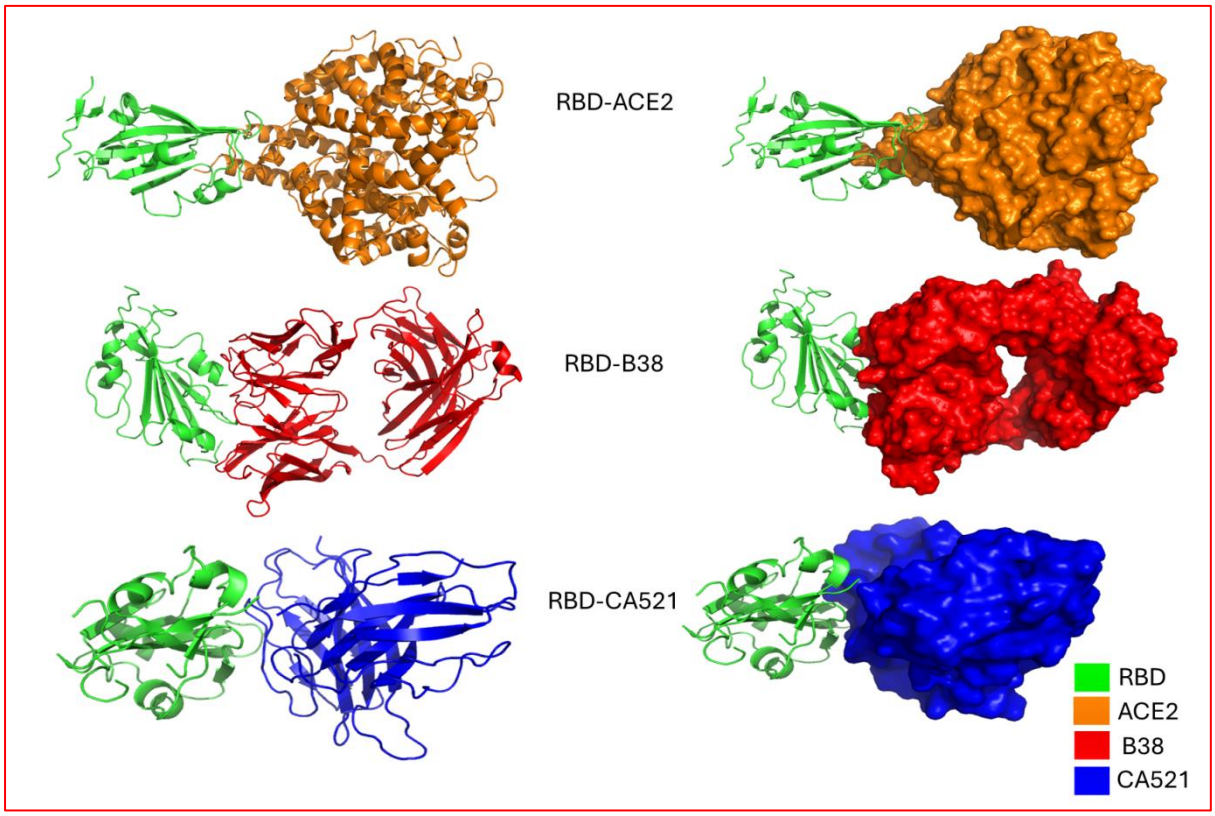

Figure 9 Protein-protein docked complexes of nCoV, with corresponding antibodies and ACE2 receptor. Color-coded keys depict the different components of docked complexes. Green: RBD; Orange: ACE2; Red: B38 antibody; Blue: CA521 antibody.

2026, Vol. 3
doi:10.x/journal.x.x.x

Table 1 Molecular properties of selected antiviral drugs and monoclonal antibodies for binding analyses with RBD of Omicron and nCoV.

S.NO	Name	Molecular formula	Molecular weight (g/mol)	Structure	Type
1	Remdesivir	$C_{27}H_{35}N_6O_8P$	602.6	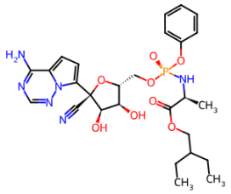	Antiviral drug
2	Atazanavir	$C_{38}H_{52}N_6O7$	704.9	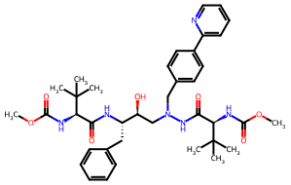	Antiretroviral protease inhibitor
3	Indinavir	$C_{36}H_{47}N_5O4$	613.8	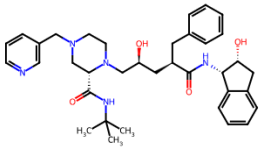	Antiretroviral protease inhibitor
4	Lopinavir	$C_{37}H_{48}N_4O_5$	628.8	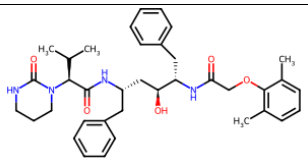	Antiretroviral protease inhibitor
5	Molnupiravir	$C_{13}H_{19}N_3O_7$	329.31	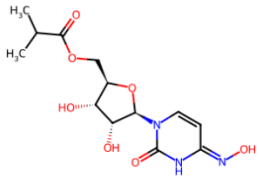	Antiviral prodrug
6	Favipiravir	$C_5H_4FN_3O_2$	157.10	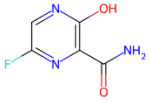	Antiviral drug
7	Oseltamivir	$C_{16}H_{28}N_2O_4$	312.40	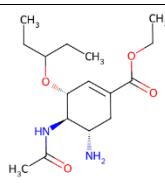	Antiviral drug

8	Ribavirin	$C_8H_{12}N_4O_5$	244.20	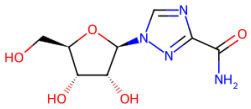	Antiviral drug
9	B38	NA	NA	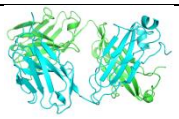	MAb
10	CA521	NA	NA	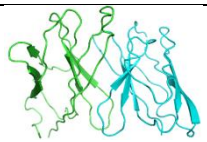	MAb

Table 2 Secondary structure elements (SSE) assessment of spike protein among emerged variant of concern (VOCs) of SARS-CoV-2.

SARS-COV-2 Variant	Alpha helix (Hh) (%)	Extended strand (Ee) (%)	Beta turn (Tt) (%)	Random coil (Cc) (%)
nCoV	26.86	21.97	5.12	46.04
Alpha (B.1.1.7)	27.70	21.71	4.44	46.15
Beta (B.1.351)	26.79	21.97	4.66	46.58
Gamma (P.1)	27.12	22.37	4.52	45.99
Kappa (B.1.617.1)	27.67	22.06	3.82	46.45
Delta (B.1.617.2)	27.09	21.86	4.22	46.84
Omicron (B.1.1.529)	29.43	21.64	3.54	45.40

Table 3 Amino acid sequence details in structural domain of spike protein in different variant of concern (VOCs).

S.NO	Spike protein of SARS-CoV-2	PDB ID	Structural domain	Amino acid range
1	nCoV	6VSB	NTD	13-304
			S1-RBD	319-541
			S1/S2	543-1208
2	Omicron	7T9K	NTD	13-301
			S1-RBD	330-513
			S1/S2	540-1205

Table 4 Binding affinity assessment of antiviral drugs and RBD (nCoV and Omicron) to understand the molecular interactions.

RBD-docked complex		Binding affinity (Kcal/Mol) (Mean ± SD, n = 3)	Interactive Amino acid residues	Chemical bonding
Omicron (7T9K)	Remdesivir	-6.2 ±0.19	SER-494,SER-496,ARG-498,TYR-501	H-bond
	Atazanavir	-6.6 0.28	LEU-517	H-bond
	Indinavir	-7.4 ±0.06	ARG-355, ASP-428, THR-430, SER-514, GLU-516	H-bond
	Lopinavir	-5.2 ±0.26	ASN-360,CYS-525	H-bond
	Molnupiravir	-5.8 ±0.31	ARG-454,ARG-457,SER-459,GLU-471	H-bond
	Favipiravir	-5.9±0.61	GLU-340, ARG-346, ASN-354,SER-399	H-bond
	Oseltamivir	-5.3±0.79	ASN-331, ASN-334, VAL-362	H-bond
	Ribavirin	-5.9±0.26	PRO-330, THR-333,VAL-362,LYS-528	H-bond
nCoV (6VSB)	Remdesivir	-7.4±0.43	PHE-6, SER-37	H-bond
	Atazanavir	-8.1±0.22	ASN-7, SER-35	H-bond
	Indinavir	-8.0±0.11	ALA-36	H-bond

	Lopinavir	-8.8±0.55	ALA-27, ALA-143	H-bond
	Molnupiravir	-6.7±0.78	PHE-6, ASN-7, VAL-31	H-bond
	Favipiravir	-5.7±0.64	ALA-27, TYR-29, LEU-54, PHE-56,THR-144	H-bond
	Oseltamivir	-6.6±0.37	PHE-2, GLY-3, ASP-28	H-bond
	Ribavirin	-6.3±0.87	ASP-62, TYR-87, ASP-92, THR-94, SER-135	H-bond

Protein-protein Complex	Docking score	
	Center	Lowest energy
*nCoV-RBD-ACE2	-648.6	-703.1
Omicron-RBD-ACE2	-846.2	-846.2
*nCoV-RBD- B38	-706.8	-924.0
Omicron-RBD- B38	-728.0	-873.7
*nCoV-RBD- CA521	-139.4	-162.6
Omicron-RBD- CA521	-836.6	-930.7

Table 5 Protein-protein docking scores of RBD and other proteins.

* Complexes were utilized as a reference.